Front. Phys. China (2007) 1: 109－124
DOI 10.1007/s11467-007-0006-7

REVIEW ARTICLE

FANG Jin-qing, BI Qiao, LI Yong

Advances in theoretical models of network science

Abstract In this review article, we will summarize the main advances in network science investigated by the CIAE Group of Complex Network in this field. Several theoretical models of network science were proposed and their topological and dynamical properties are reviewed and compared with the other models. Our models mainly include a harmonious unifying hybrid preferential model, a large unifying hybrid network model, a quantum interference network, a hexagonal nanowire network, and a small-world network with the same degree. The models above reveal some new phenomena and findings, which are useful for deeply understanding and investigating complex networks and their applications.

Keywords theoretical model of network science, a harmonious unifying hybrid preferential model, a large unifying hybrid network model, quantum interference network, topological and dynamical properties

PACS numbers 89.75.-k, 89.75.Da, 89.75.Fb

1 Introduction

In 1998, Watts and Strogatz (WS) proposed the small world (SW) model [1, 2] and in 1999 Barabasi and Albert (BA) proposed the scale-free (SF) model [3, 4]. These two discoveries of the SW effect and the SF property symbolized that complex network research has broken through the imprisonment of random graph analysis that started in the 1960s. Since then, interdisciplinary studies and conferences on complex networks have become a very hot activity all over the world. In the last decade, people have witnessed the great progress of complex networks. It was a very pleasant news [5] from the University of Notre Dame on August 24, 2006, that Barabasi was awarded a computing medal, which was presented by the Hungarian von Neumann Computer Society for outstanding achievements in computer-related science and technology. This is because Barabasi is a pioneer in the field of networking as a unified science and author of "Linked : The new science of network."

Complex networks, which belong to network science, have emerge all over the place in nature and in society, including physical, social, informative and technological networks. A variety of theoretical models of networks have been proposed and investigated in various literatures [1–20]. Most of the real world networks (RWNs) are characterized by both the SF and the SW effects, which have power law of the degree distribution, relatively small average path lengths (APL) and high average clustering coefficients (ACC). However, one of the most important problems at present in network science is that the majority of the research concentrates on the BA network and its varieties [3–19], which introduces random preferential attachment (RPA) mechanism to mimic un-weighted growing networks. But many current models are not completely consistent with those ubiquitous properties in RWNs although they have been useful at reproducing features to approach the RWNs. As pointed out by well-known American scientist Wilson [13, 14], "The greatest challenge today, not just in cell biology and ecology but in all of science, is the accurate and complete description of a complex system. Scientists have broken down many kinds of systems. They think they know most of the elements and forces. The next task is to reassemble them. At least in a mathematical model that captures the key properties of the entire ensemble." That is the total motivation for this review article based on our work.

The article is organized as follows. In Section 2, we shall briefly review the main models of current network science. In Section 3, a harmonious unifying hybrid preferential model (HUHPM) and main numerical and analytical results are given briefly. In Section 4 the HUHPM is extended to a large unifying hybrid network model (LUHNM) and fresh

FANG Jin-qing (✉), BI Qiao, LI Yong
CIAE Group of Complex Network, China Institute of Atomic Energy, P.O. Box 275-81, Beijing 102413, China
E-mail: fjq96@126.com

Received November 30, 2006

results are shown. In Sections 5 and 6, the quantum interference network and the hexagonal nanowire network are summarized, respectively. In Section 7, the SW model with the same degree is mentioned. Lastly, a summary of the article is made.

2 Brief review on current main models of network science

Most models of network science can be found in Refs. [1–5, 7–16] and the references therein, which include the original detail properties of topology and dynamics, and have a better review. In this article, from our point of view, we will only give the classification of the complex networks and most models of network science so far. Then we pay attention to focus our recent work in this field. The current main models may be classified into different types of complex networks, as shown in Table 1, such as: social network, information network, technological network, biological network and so on. There are random graph, small-world network, scale-free network and hybrid network (e.g., LUHNM). Especially, we can classify the networks into two categories: un-weighted networks and weighted networks, in which the random graphs, generalized random graphs, static SF networks and evolving SF network, all these belong to the generalized random networks, they always ignore deterministic linking, but another extreme case is that *only* consider *determinism* instead of random. These two extreme cases are useful for theoretical analysis easily and reproduce the main topological properties for the RWNs. However, based on the foundational observation fact for a unifying world in natural and social networks, one cannot ignore anyone of order and random. As a matter of fact, the interactions in the real world are neither completely regular nor completely random and

Table 1 Classification of complex networks and models of network science.

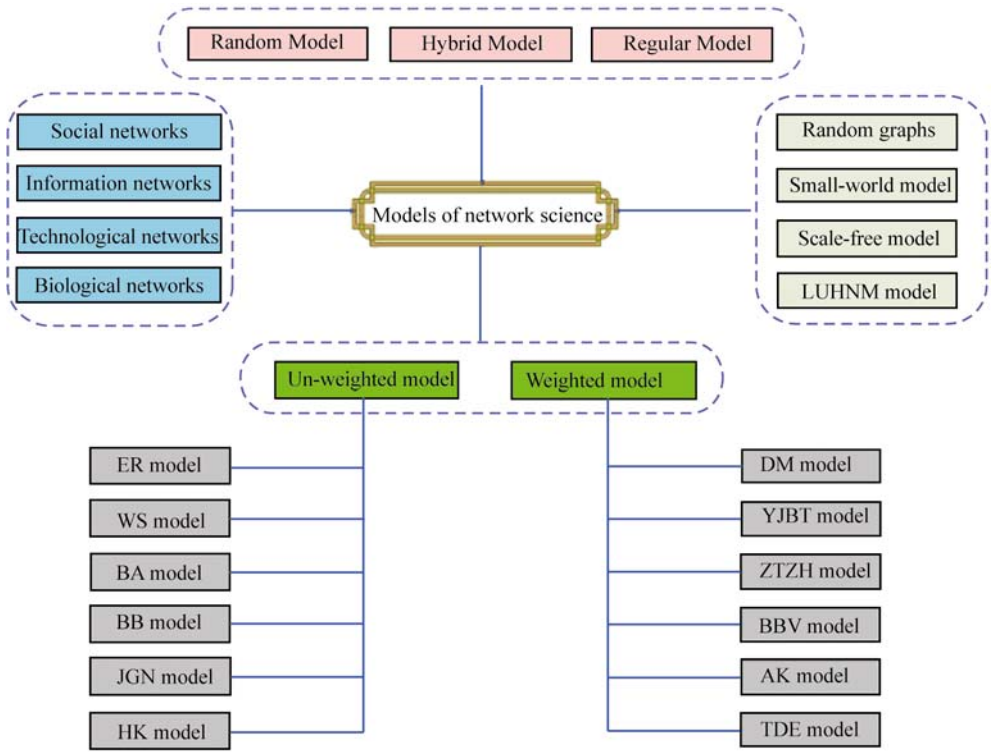

A list of model names and corresponding references:

ER: P. Erdös and A. Rényi, Publ. Math. Debrecen, 1959, 6: 290
WS: D. J. Watts and S.H. Strogatz, Nature,1998, 393: 440
BA: A. -L Barabási and R. Albert, Science, 1999, 286: 509
BB: G. Bianconi and A. -L. Barabási, Europhys. Lett., 2001, 54: 436
JGN: E. M. Jin, M. Girvan, and M. E. J. Newman, Phys. Rev. E, 2001, 64: 46132
HK: P. Holme and B. J. Kim, Phys. Rev. E, 2002, 65: 26107
LUHNM: Fang J. Q. and Bi Q., Proceedings of 2006 National Conference on Complex Networks, Wuhan, November 16–18, 2006: 6; Fang J. Q. and Liang Y., Chin. Phys. Lett., 2005, 22: 2719; Lu X. B., Wang X. F., and Fang J. Q., Physica A, 2006, 371: 841
DM: S. N. Dorogovtsev and J. F. F. Mendes, Europhys. Lett., 2000, 52: 33
YJBT: S. H. Yook, H. Jeong, A. -L. Barabási, and Y. Tu, Phys. Rev. Lett., 2001, 86: 5835
ZTZH: D. Zheng, S. Trimper, B. Zheng, and P. M. Hui, Phys. Rev. E, 2003, 67: 040102
BBV: A. Barrat, M. Barthélemy, and A. Vespignani, Phys. Rev. Lett., 2004, 92: 228701
AK: T. Antal and P. L. Krapivsky, Phys. Rev. E, 2005, 71: 026103
TDE: Wang W. X., Wang B. H., Hu B., Yan G., and Ou Q., Phys. Rev. Lett., 2005, 94: 188702

lying between the extremes of order and randomness. The world should be harmoniously unified. Most network models focus on the un-weighted network, which may reflect the most topological characteristic and dynamical behavior between the network nodes and connectivity, but they could not describe the strength of interaction and difference of connected edges in the RWNs. Various weights and strength almost exist in the RWNs and the weighted networks can carefully portray the nodes connection and mutual interaction that not only reflect the topology of the RWNs, but also reveal the physical and dynamic characteristics for the RWNs.

Recently, as given in Table 1, several weighted networks have been proposed in the literature, in which one of typical weighted models is the BBV model, the weighted evolving network model [23, 24]. The BBV model yields the SF properties of the degree, weight and strength distributions, but its weight dynamical evolution is triggered only by newly added vertices, resulting in few satisfied interpretations to the collaboration networks and the transport networks (e.g., airline systems). The other is the TDE model for technological networks [25], they considered two coupled mechanisms: topological growth and the strengths' dynamics, which is suitable for technological networks. However, both the BBV and the TDE models consider *only random preferential* attachment (RPA), and does not consider the deterministic preferential attachment (DPA) and other possible linking way. This is in contradiction to the fundamental observation in which one can see both the RPA and the DPA, in general, the deterministic and the random factors exten sively exist in our unifying real-world. To improve the above models, we have proposed a large unifying hybrid network model (LUHNM), which includes the harmonious unifying hybrid preferential model. We will summarize these two models as follows.

3 Harmonious unifying hybrid preferential model (HUHPM)

From our analysis and point of view, as seen above, we confirm that one cannot ignore RPA and DPA, which should be a harmonious unifying one in theoretical models for dedicating the real-world. Certainly, the combination of RPA with DPA should be considered and investigated in the growing and evolving complex networks. Motivated by this goal, we first propose a hybrid preferential model for unweighted and weighted complex networks [26–29], which are extended to a harmonious unifying hybrid preferential model (HUHPM), in which only total hybrid ratio *d/r* is introduced as a key control parameter, and is used to master the topological and dynamical properties in complex networks. We then applied the HUHPM to the un-weighted BA, the weighted BBV and the TDE models; corresponding networks are called the HUHPM-BA network, the HUHPM-BBV network and the HUHPM-TDE network, respectively. Through both theoretical analysis and numerical simulation, it was found that the HUHPM has a series of universal properties, which approaches the RWNs and is more suitable for most un-weighted and weighted networks. In the following subsections we will summarize the main idea and the important results.

3.1 Idea and method

The HUHPM is expressed simply as:

$$\boxed{\text{HUHPM}} = \begin{array}{c}\boxed{\text{Random preferential attachment and growing way for any model}} \\ + \\ \boxed{\text{Deterministic preferential attachment or other connective way}}\end{array}$$

This means that the HUHPM can rest on any type of network's original growth way and RPA pattern by adding the DPA pattern according to arrangement of the degree distribution from the largest to the smallest value (and may also broadly develop other determination connection methods). This implementation combines the random connection with the determination connection by using the total hybrid ratio to request the growth scale size of the networks. Hence, the unified hybrid ratio is defined by

$$\frac{d}{r} = dr = \frac{\text{Time intervals } d \text{ of deterministic preferential attachment (DPA)}}{\text{Time intervals } r \text{ of random preferential attachement (RPA)}} \tag{1}$$

where d and r are a number of time intervals for the DPA and the RPA, respectively. In the process of the network evolution, the total hybrid ratio d/r must maintain the same value by combining the RPA and the DPA. Actually, one can use different orders to make the two hybrids grow the network in turn, until the required scale size is achieved. The main principle for implementation of hybrid growth network is as follows:

(1) The growth way: first, use each growing rule of the model to carry on the growth by the RPA way.

(2) Growth connection way: each step adopting the kind of connection mechanism must accord to the hybrid ratio d/r.

(3) DPA way: After each RPA, rank of the degree of nodes is reordered again from the biggest to the smallest: $k_1 > k_2 > \cdots > k_m > \cdots > k_n$, then m nodes is attached preferentially. This is a general way for the DPA.

We have applied the above idea and method to some of the current typical models [1, 21, 22] and follow the above steps to give the rules of the HUHPM-BA, HUHPM-BBV and HUHPM-TDE networks. The concrete constructions are followed by their respective preferential attachment methods [3, 4, 20, 21, 23–25].

After the procedures above have been completed for each model, the rank of the vertices degrees is then rearranged from the largest to the smallest as $k_1 > k_2 > \cdots > k_n$. The DPA is to be conducted for d time steps for the HUHPM networks

according to the new rank of the vertices degrees above when choosing the nodes connected to the new node. This procedure creates a network with $N = r + d + m_0$ nodes.

The steps (1)–(3) of the HUHPM algorithm are repeated again. Two kinds of preferential attachments are applied in turns under a certain hybrid ratio *d/r*, until finally reaching the desired size of the network.

The main results of HUHPM are briefly given as follows.

3.2 Power-law exponents sensitive to hybrid ratio *d/r*

The relations of the power-law exponents with the total hybrid ratio *d/r* for different typical networks have been investigated using both simulation and analysis. For the HUHPM-BA network we have obtained the function relationship of power-law exponent γ with *d/r* as:

$$\gamma_{\mathrm{BA}}^{\mathrm{HUHPM}} = \frac{1}{\beta} + 1 = \frac{A_1}{\exp\left[\left(\frac{d/r}{A_2}\right)^{A_3}\right]} + A_4 \quad \text{(formula 1)} \quad (2)$$

If adjusting relevant parameters, we have another function relationship for γ with *d/r*:

$$\gamma_{\mathrm{BA}}^{\mathrm{HUHPM}} = \gamma_0 + A_1 \cdot \left[1 - \exp\left(-\frac{d/r}{A_2}\right)\right] + A_3 \cdot \left[1 - \exp\left(-\frac{d/r}{A_4}\right)\right] \quad \text{(formula 2)} \quad (3)$$

where $\gamma_0 = 3$. The parameters for Eqs. (2) and (3) (formulas 1 and 2) are listed in Table 1 of Ref. [30]). As shown in Fig. 3(a), the theoretical results coincide with the numerical curves for corresponding different parameters.

Similarly, we have the relation γ and *d/r* for the HUHPM-BBV and HUHPM-TDE by considering associated weighted parameters δ and w, respectively,

$$\gamma_{\mathrm{BBV}}^{\mathrm{HUHPM}} = \frac{4\delta + \dfrac{A_1}{\exp\left[\left(\dfrac{d/r}{A_2}\right)^{A_3}\right]} + A_4}{2\delta + 1} \quad \text{(formula 3)} \quad (4)$$

and

$$\gamma_{\mathrm{BBV}}^{\mathrm{HUHPM}} = \frac{4\delta + \gamma_0 + A_1\left(1 - \exp\left(-\dfrac{d/r}{t_1}\right)\right) + A_2\left(1 - \exp\left(-\dfrac{d/r}{t_2}\right)\right)}{2\delta + 1} \quad \text{(formula 4)} \quad (5)$$

where parameters for different δ are also given in Ref. [29].

The HUHPM-TDE γ is given by

$$\gamma_{\mathrm{TDE}}^{\mathrm{HUHPM}} = 1 + \chi\left\{1 + \left[\frac{A_1}{\exp\left(\dfrac{d/r}{A_2}\right)^{a_1}} + (A_4 - 2)\right]\frac{m}{2w+m}\right\} \quad \text{(formula 5)} \quad (6)$$

and

$$\gamma_{\mathrm{TDE}}^{\mathrm{HUHPM}} = 1 + \chi \cdot \left[1 + \frac{\left\{A_1\left[1 - \exp\left(-\dfrac{d/r}{t_1}\right)\right] + A_2\left[1 - \exp\left(-\dfrac{d/r}{t_2}\right)\right] + (\gamma_0 - 1)\right\}m}{2w+m}\right] \quad \text{(formula 6)} \quad (7)$$

where the strength of the node $s \propto k^{\chi}$ and $\chi = 1$ for HUHPM-BBV and χ is related to w for HUHPM-TDE [23]. Relevant parameters A_1, A_2, A_3, A_4 are also given in Table 1 of Ref. [29, 30].

Figure 1 shows the exponent γ of degree power law versus the total hybrid ratio *d/r* by comparing the numerical simulation result with the theoretical results of Eqs. (1)–(3) for the three typical networks, (a) HUHPM-BA, compared three orders of connections (HPAS-1, HPAS-2, HPAS-3), which do not affect properties of topology; (b) the HUHPM-BBV and (c) the HUHPM-TDE, where $N = 6000$ and $m = m_0 = 3$.

Several important features are seen from Eqs. (2)–(7) and Fig. 1 wherein the theoretical results are in agreement with the numerical simulations. First, the exponents γ of the power-laws are sensitive to the change of hybrid ratio *d/r*, as a new topological characteristic. Here, the *d/r* = 1/1 is a threshold value. If $d/r \leqslant 1$, $\gamma \leqslant 3$, then γ is nearly constant, this is consistent with the RPA playing a leading role. If *d/r* >1/1, in the HUHPM-BA and the HUHPM-BBV models, γ increases as *d/r* increases. Once RPA approaches to zero (r = 0, *d/ r*), γ is very large or even approaches infinity, and the power-law then vanishes, and often concentrates on several high condense nodes. Second, the power exponents have a quite complicated relation with the hybrid ratio *d/r*, which is beyond simple relation in the corresponding original models. This reflects either a mutual competition or a harmonious unification between the DPA and the RPA. Thirdly, the HUHPM-BBV and HUHPM-TDE models are related to weight associated parameter δ or w, respectively, which is closely connected to the architecture producing the network. This makes the relationship more complicated. For the three typical networks, (a) HUHPM-BA, (b) HUHPM-BBV, and (c) HUHPM-TDE, under their different parameters, the simulation results are consistent with the theoretical results. Finally, similar results for the power-laws of the node strength and the edged weight governed by the total hybrid ratio *d/r* are also obtained in the HUHPM-BBV and HUHPM-TDE [30].

3.3 Effect of *d/r* on the SW properties

The SW effect in the HUHPM is much better than the other models since it has the shortest APL (L) as well as the largest ACC (C). Taking the HUHPM-TDE model with w < 1 as an example, as shown in Fig. 2, in which when $w = 0$, the HUHPM-TDE reduces to HUHPM-BBV. The APL value

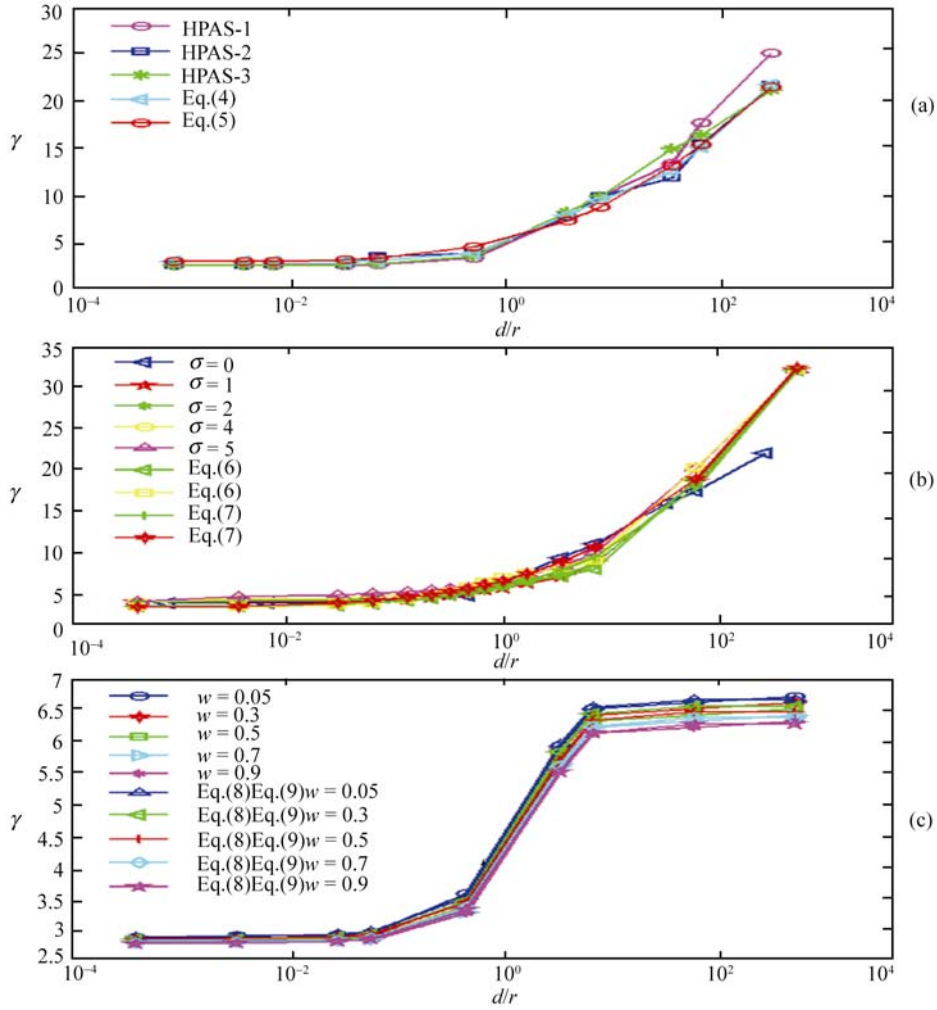

Fig. 1 The exponent γ of power-law versus the d/r compared simulation results with theoretical results of Eqs. (1)─(3). **(a)** The HUHPM-BA, compared three orders of connections (HPAS-1, HPAS-2, HPAS-3), which do not affect the values of exponents; **(b)** The HUHPM-BBV, compared different values of weight parameter δ [24, 25]; **(c)** The HUHPM-TDE compared different values of weight parameter w [26]. Here $N = 6000$ and $m = m_0 = 3$.

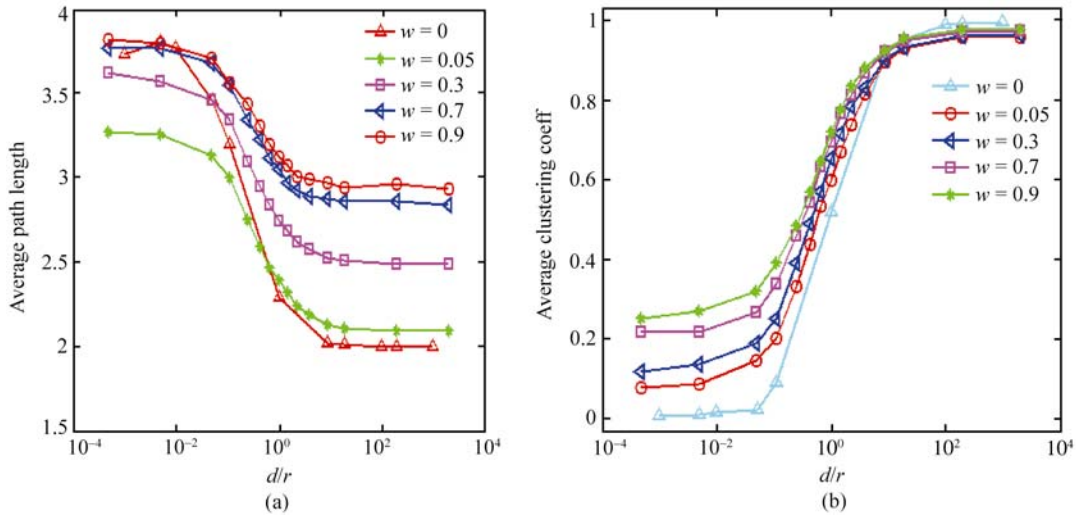

Fig. 2 **(a)** APL vs d/r; **(b)** ACC vs d/r under different values of weight parameter $w < 1$ for HUHPM-TDE. Here $N = 6000$ and $m = m_0 = 3$.

increases as w increases. If $w > 1$, when d/r increases, w increases, the APL also becomes smaller, this fully explains that HUHPM can cause the small world effect, which is more close to the actual network than the other models, as demonstrated and compared later.

Theoretically, we derive the relation of the APL with exponent γ for the HUHPM-TDE model:

$$L_{\mathrm{TDE}}^{\mathrm{HUHPM}} = \frac{1}{2} + \frac{\ln\dfrac{9}{\gamma-1} - \dfrac{2}{9(\gamma-1)} + 8.6192}{4.788} \tag{8}$$

For the HUHPM-BA and the HUHPM-BBV networks similar relationships are also obtained [30].

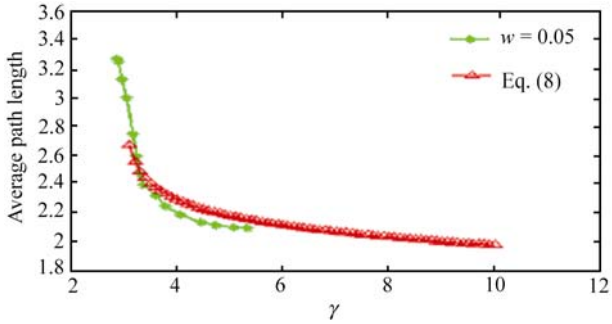

Fig. 3 Comparing theoretical result with numerical simulation for the HUHPM-TDE. Here $N = 6000$, $w = 0.05$ and $m = m_0 = 3$.

Furthermore, by comparing the APL with the network size N for the three kinds of models, which are the HUHPM, the original BA model and random graph model, Fig. 4(a) shows the APL of the HUHPM-BA to be the shortest. The red (*block*) is the result of a random graph model; its APL value is the largest, blue (*dot*) is the result of the original BA model, whose L value is the second biggest. The green (*asterisk*) is the result of Eq. (60) in Ref. [10], whose L value is in the middle. The brown (*triangle number*) is the HUHPM-BA result; L value is the smallest. This explains once more that the HUHPM can reduce the APL under the same level size N, which is able to achieve the smallest APL compared with other networks.

Similarly, Fig. 4 (b) shows comparing the average clustering coefficient (ACC) C with the network size N for the three kinds of models, which are the HUHPM, the original BA model and the random graph model. One can see that the C of HUHPM is largest, where the brown (*block*) is the result of the random graph model, its C value is the smallest; the red (*dot*) is the result of the original BA model, whose C value is the second biggest; the green (*asterisk*) is the result of HUHPM-BA, whose C value is the largest. This explains once more that the HUHPM can really enhance the C under the same level size N, which is able to achieve the biggest C compared with other model networks.

In addition, we have also investigated the effect of the hybrid ratio d/r on dynamical synchronizability for the HUHPM networks in Ref. [27].

The results above show that all characteristics of the HUHPM models are closer to the RWNs, which have the SF as well as WS properties. The results imply that although the

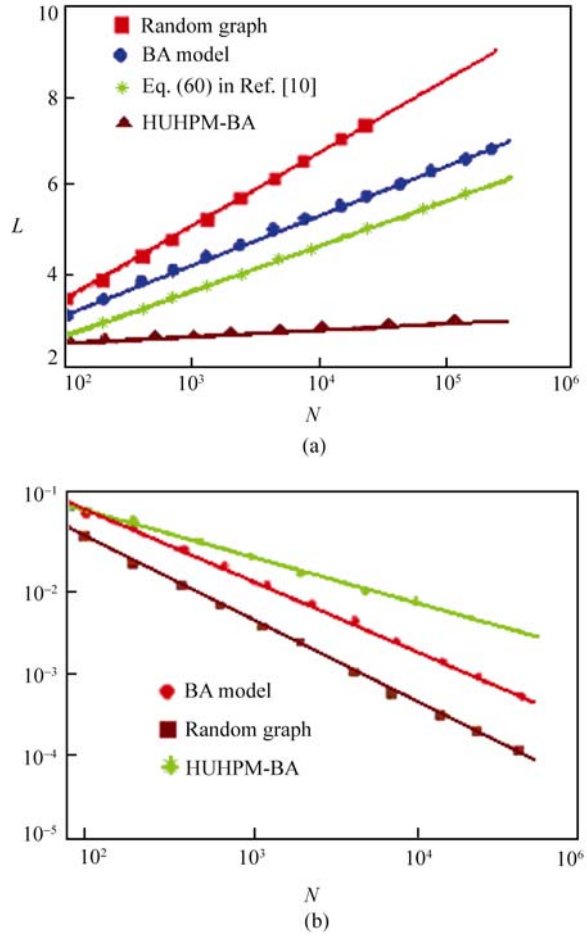

Fig. 4 Comparing SW effects of the HUHPM with other models. **(a)** illustrates that when $d/r = 1/1$ and $\langle k \rangle = 4$, using the HUHPM-BA method to obtain L is shortest, the brown (*triangle number*) is the HUHPM-BA result; the green (*asterisk*) is the result of the Eq. (60) in the literature [10]; the blue color (*circular number*) is the result of the original BA model; red (*block number*) is the result of random graph; **(b)** is a similar comparison between C and N for the HUHPM-BA, random graph and original BA models.

RPA is the main mechanism to produce the distributed power law function, the combination of the RPA with the DPA has more rich transition features between random and order. Therefore, the DPA also displays a vital role, including the ability to suppress the power distributed heavy tail. The HUHPM models can cause randomness and determinism to arrive at the harmonious unification only controlled by total hybrid ratio.

4 Large unifying hybrid network model

The shortcoming of the HUHPM above is that it considers *only preferential* attachments and could not explain *why* social networks are mostly positive degree-degree correlated (assortatively mixed) while biological and technological networks tend to be negative degree-degree correlated (disassortative). Could one give a unification explanation? Be-

cause the degree-degree correlation is another important property in complex networks, as Newman emphasized [13, 14], "there is an important element missing from these models: many networks show 'assortative mixing' on their degree, i.e., a preference for high-degree vertices to attach to other high-degree vertices, while others show disassortative mixing — high-degree vertices attach to low-degree ones." Of the social networks studied all have positive degree-degree correlation r_c. In contrast, the technological and biological net-works are all of the negative degree-degree correlation. To answer the above questions, Wang *et al*. proposed a mutual attraction model (MAM) to characterize the weighted evolving networks [15], by introducing the initial attractiveness A and the general mechanism of the mutual attraction, and assume the connectivity probability $\Pi_{i\to j}\dfrac{(s_j+A)}{\sum_{k\neq i}(s_k+A)}$. The $A > 0$ in the MAM governs the probability for "young" nodes to get new links and weights, and obtain tunable degree assortativety, depending on the values of m and A. But in the MAM the tunable range of the r_c value is very small, as seen in Fig. 6 (b), the maximum value is only about 0.2 although the two parameters (A, m) are changed from 1 to 12 significantly. So the questions also raised here is: Why is the r_c value so small in the MAM? Is it consistent with the RWNs completely? The results of the MAM mimics both the assortative and disassortative of the weighted evolving networks but its description is incomplete because of only producing small values of disassortative r_c . In fact the physics co-authorship and film actor collaborations networks have r_c = 0.363 and 0.276 [13, 14], respectively. Clearly, the MAM does not completely catch all the key mechanisms behind the various complex networks yet, and even more importantly, the factors that must effect r_c strongly may have been ignored.

To explore and solve the problem above, we can make a careful analysis and then find that the main problem of the theoretical models above is that they consider *only random preferential* linking as a key formation mechanism but ignore any other possible linking ways that can largely affect the structure and dynamics of complex networks. Although the HUHPM above considered mixing random with the deterministic, it was *only* limited to *preferential* attachment. Furthermore, for improvement of the HUHPM, we have proposed a large unifying hybrid network model (LUHNM), which is controlled by the three hybrid ratios in different levels. Through the study of numerical simulation and theoretical analysis, we find that the LUHNM has included the most possible previous and current models of network science. It is found from the LUHNM that it has new phenomena and fresh nontrivial properties, which can give satisfactory answers and worthwhile for more unified mechanisms of complex networks, and can have reasonable explanation for some problems.

4.1 Basic idea and method of the LUHNM

The HUHPM has unified both the RPA and the DPA, but "*preferential* attachment" is not necessary completely in various networks, including social networks and technological networks and so on, because any networks may have two or more possible hybrid linking ways: general, preferential and special linking for both random and order. To describe the RWNs and improve the HUHPM, we extend the HUHPM to a large unifying hybrid network model (LUHNM) [31], as shown in Fig. 5.

In the LUHNM, three-level hybrid ratios are defined respectively. At the first level, the total hybrid ratio d/r, Eq. (1) is changed to

$$dr = \frac{d}{r} = \frac{\text{Total time intervals of deterministic attachment (DA)}}{\text{Total time intervals of random attachment (RA)}} \tag{1′}$$

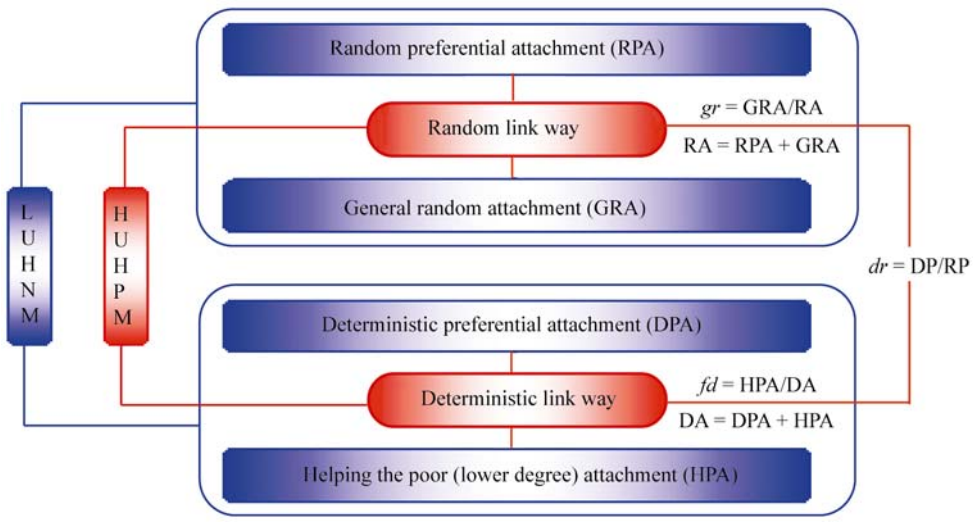

Fig. 5 Diagram of physical idea of the LUHNM.

At the second level, there are two hybrid ratios, one is a deterministic hybrid ratio *fd*, which is defined by

$$fd = \frac{f}{d} = \frac{\text{HPA}}{\text{DA}} \tag{9}$$

where HPA is helping poor attachment, DA = HPA + DPA.

The other is a random hybrid *gr*, which is defined by

$$gr = \frac{g}{r} = \frac{\text{GRA}}{\text{RA}} \tag{10}$$

where GRA is a general random attachment, RA = GRA + RPA.

In the evolving process of the complex networks, the total hybrid ratio *dr* must maintain the same value by combining the RA and the DA, but there are two other mixing ways, the RA including *gr* and RPA, and the DA including *fd* and DPA, respectively. Actually, multiple hybrid kinds of attachments carried on is very flexible for the LUHNM. It is notable that the general case of the LUHNM is of *fd* and *gr* in the range of (0, 1), which includes the most important kinds of network models:

(a) *fd* = 1/1: complete helping poor attachment (HPA) for the DA, instead of the DPA.

(b) *fd* = 0/1: complete DPA for the DA, instead of the HPA.

(c) *gr* = 1/1: complete GRA for the RA, instead of the RPA.

(d) *gr* = 0/1: complete RPA for the RA, instead of the GRA.

(e) *fd* = 0/1 and *gr* = 0/1: it reduces to the HUHPM.

(f) *fd* = 0/0 and *gr* = 0/1: it reduces to the BA, the BBV and the TDE models.

(g) *fd* = 0/0 and *gr* = 1/0: it reduces to the ER model.

(h) *fd* ≠ 0 and *gr* = 0/0: it reduces to complete deterministic model.

It can be seen clearly from the 8 kinds of models above that the LUHNM is a reasonable, natural and large unification for most of the network models in both theory and practice, i.e., one can rest on any type of network model and pattern formatted by the combination of 3 different ratios (*dr, fd* and *gr*) to grow and govern network scale-size as needed. This means that one can combine a different hybrid to grow the network in turn, until the required scale size is achieved. On the other hand, this implementation combines the random connection with the determination connection by using the multiple hybrid ratios according to the need. Thus, one can have certain diverse and complex networks.

4.2 Degree-degree correlation versus total hybrid ratio *dr*

The main results of the degree-degree correlation r_c versus *dr* and *m* for the LUHNM are shown in Fig.6 under different values of *dr*, *gr*, and *fd*. It is found that the LUHNM reveals two interesting transition features of degree-degree correlation from negative to positive in an un-weighted network. First, as shown in Figs. 6 (a), (c)–(f), *only if* the *fd* ⩾0.9/1, which means helping the poor attachment (HPA) for the DA is dominated strongly, whatever the value of *gr* is, the r_c curve exists as one peak or mutual peaks (one or more extreme values), which is a new phenomenon, compared to the MAM model [15] shown in Fig.6 (b) and other models, and is closely associated with *d/r* and *m*. Second, as the *dr* increases the r_c increases and reach a large positive value to about 0.7. It seems that the *fd* increases and approaching 1/1 is a necessary condition for having the extreme and large r_c value. This finding can explain the question above.

4.3 Degree-degree correlation r_c versus *fd* and *gr*

Under a different typical region of the total hybrid ratio *dr,* the r_c vs *gr* and *fd* are shown in Fig.7.

From Fig.7, we can obtain the linear fit relation of r_c with *gr* and *fd*:

$$r_c = a_1(gr) + b_1, \quad gr \in [0,1] \tag{11}$$

When *dr* is smaller, the relation of r_c with *fd* is approximately linear:

$$r_c = a_2(gr) + b_2, \quad gr \in [0,1] \tag{12}$$

For the *dr* < 1/1, $a_1 > 0$; as the *dr* increases, a_1 decreases; If $dr \to N$, $a_1 \to 0$. For the *dr*⩾ 1/1 and $fd \to 1$, the relationship above is strongly changed to:

$$r_c = \begin{cases} a_1 e^{fd/\alpha} + a_2, & 0 \leqslant fd \leqslant 0.9 \\ b_1 + \dfrac{2b_2 b_3}{\pi[4(fd - b_4)^2 + b_5^2]}, & 0.9 \leqslant fd \leqslant 1 \end{cases} \tag{13}$$

where a_i and b_j are some parameters to be determined, i = 1, 2, 3; j = 1, 2, 3, 4.

We can see from Fig.7 and Eqs. (11)–(13) that there are three regions of *dr* value and results: (1) When *dr* ⩽ 1/99, where random is dominant, the *r* increases linearly as the *gr* and *fd* increases. (2) When *dr* = 1/1, which is a transition point, because it is evenly matched in strength for random and deterministic linking, the r_c increases slowly as the *gr* increases, the r_c increases linearly if *fd* ⩽ 0.9/1 *but* the r_c is *abruptly* increased *only if* the *fd* ⩾ 0.9/1. (3) When *dr*⩾ 99/1, deterministic linking is dominant, the r_c increases much more slowly as the *gr* increases, but the r_c is *still abruptly* increased *only if* the *fd* ⩾ 0.9/1. These results imply that the *fd* ⩾ 0.9/1 plays a key role for the degree-degree correlation transition although sometimes the *gr* value also has important effects. The transition features depend on their matched sense of 3 different hybrid ratios. Therefore, the LUHNM can give a reasonable answer to some questions above for complex RWNs. For example, why are social networks mostly positive degree-degree correlated (assortatively mixed) while biological and technological networks tend to be negative degree-degree correlated (disassortative)? Using our findings above, it can easily be understood that the two situations can also take place in any RWNs. Since 1980' Chinese government has proposed and implemented a

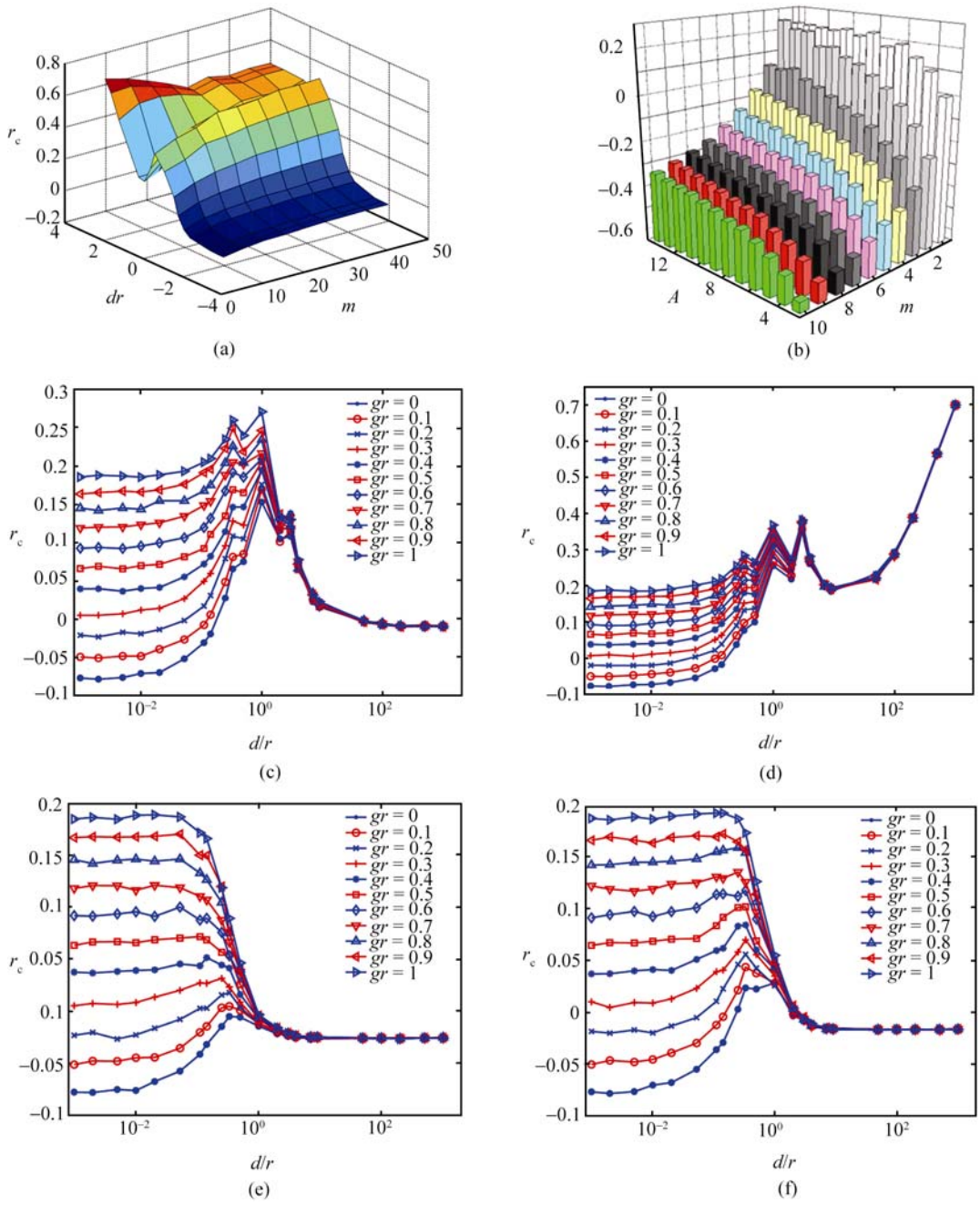

Fig. 6 The r_c versus dr for the LUHNM and compared with the results of the MAM [15]. **(a)** and **(c)**–**(f)** under different fd and gr, in the LUHNM; **(b)** The results of Ref. [13]; **(c)** fd = 0.99/1; **(d)** fd = 1/1; **(e)** fd = 0.95/1; **(f)** fd = 0.97/1.

so-called "policy of helping the poor region" and "Chinese eastern supporting Chinese western region", that want to use advanced technology and fund in eastern region to support the western region, in which case the LUHNM should put into increasing fd value , then makes increasing the r_c value. Trough such a growing mechanism Chinese people may lead to be on route of common rice and to construct a harmonious society. Therefore, the policy above accords with the LUHNM. The LUHNM can also be applied to research the entrepreneurial economy based on complex ecological network.

4.4 Complexity of degree-degree correlation in weighted LUHNM

In the last subsection, we will only give the main results of the un-weighted LUHNM. As a matter of fact, the weight effect is over almost all networks and is of significance for the RWNs. Therefore, we have also investigated the transi-

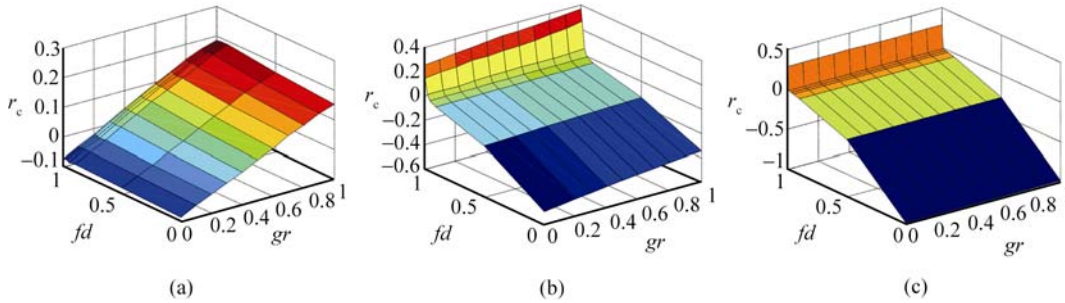

Fig. 7 The r vs gr and fd under three typical total hybrid ratio. **(a)** dr = 1/99, **(b)** dr = 1/1, and **(c)** dr = 99/1.

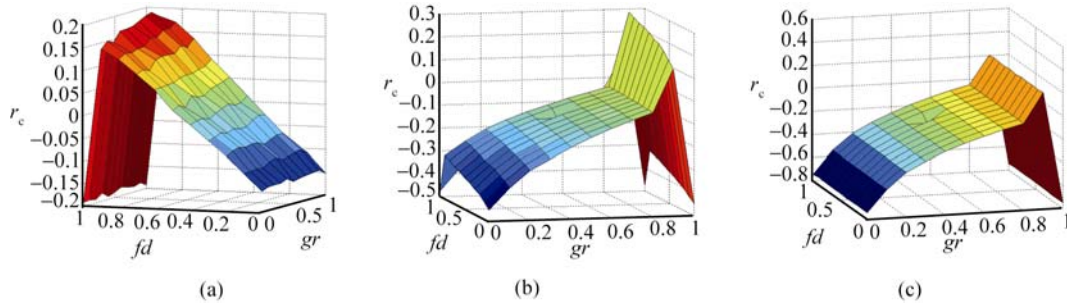

Fig. 8 Some results r versus fd and gr for the weighted LUHNM. **(a)** dr = 1/99; **(b)** dr = 1/1; **(c)** dr = 99/1.

tion complexity of degree-degree correlation for the weighted LUHNM [31]. Some results of the weighted LUHNM for the three typical total hybrid ratio are given in Fig. 8. From Fig. 8, we see that a much more complex relation exists than the un-weighted LUHNM; not only does the r_c curves appear as mutual peaks but it also increases nonlinearly as the fd and gr increase.

In conclusion, either the un-weighted or the weighted LUHNM can reveal some nontrivial properties of topology and dynamics. Therefore the LUHNM can give a reasonable answer for the questions raised above, especially for social networks, which are mostly positive degree-degree correlated, while biological and technological networks tend to be negative degree-degree correlated if we change the three hybrid ratios in the LHUNM. It is easily understood that the different correlation can take place in the RWNs.

5 A quantum information network

The network characteristic in the quantum microcosm can be explored, especially studies of the topological property of quantum information network (QIN) and its application, but this aspect has not yet been seen in the related literature. We have proposed a QIN whose spatially separated nodes are connected by the quantum communication channel (QC) [32–34]. The QC and operation between the different nodes allow the network to perform various QC non-locally. The photon transmits interaction between the two separate network nodes in the channel as the flight ebit or tangled ebit to perform the quantum logic computation or the QC. As an example, the QIN schematic drawing is shown in Fig. 9, where we suppose that the QIN nodes consist of a trapped-atom inside a high-Q cavity. The atom has a standard "Λ" type of internal state, the ebits are flying polarization-entangled photons. Because the user is stochastic, the environment noise is stochastic, therefore we consider that the QIN node and the segment fluctuation is stochastic also.

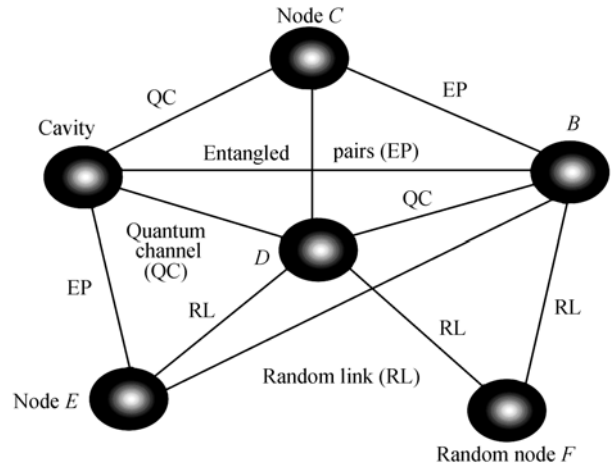

Fig. 9 A schematic quantum information network.

We constructed a QIN with Gaussian channel (GC). Although there is a strong coupling between the photons emitted from the atoms confined in the cavity, the encoded information carrier in the channel are photons which may interact with the environmental field at temperature T. This is

a typical quantum Brownian motion problem. In the coherent representation, a quantum Fokker-Planck equation (FPE) for QID $f(\alpha,\alpha^*,t)\ln f(\alpha,\alpha^*,t)$ is obtained by

$$\begin{aligned}&\frac{\partial}{\partial t}f(\alpha,\alpha^*,t)\ln f(\alpha,\alpha^*,t)\\&=\left[\left(\frac{r_0}{2}+\mathrm{i}\omega_0\right)\frac{\partial}{\partial\alpha}\alpha+\left(\frac{r_0}{2}-\mathrm{i}\omega_0\right)\frac{\partial}{\partial\alpha^*}\alpha^*\right.\\&\left.+r_0N\frac{\partial^2}{\partial\alpha\partial\alpha^*}\right]f(\alpha,\alpha^*,t)\ln f(\alpha,\alpha^*,t)\end{aligned}\tag{14}$$

where $|\alpha\rangle$ is a coherent state, ω_0 is frequency of a harmonic oscillator, N is the mean number of quanta in the mode with ω_0, γ_0 is defined as $\gamma_0\equiv\mathrm{i}\pi|\eta_k|^2$, here η_k denotes the coupling between the oscillator and kth field mode. The solution of the FPE is found as:

$$\begin{aligned}&f(\alpha,\alpha^*,t)\big|_{(\alpha_0,\alpha_0^*,0)}\\&=\frac{1}{\pi N(1-\mathrm{e}^{-r_0t})}\exp\left[-\frac{(\alpha-\alpha_0\mathrm{e}^{-\frac{r_0}{2}t}\mathrm{e}^{-\mathrm{i}\omega_0t})^2}{N(1-\mathrm{e}^{-r_0t})}\right]\end{aligned}\tag{15}$$

The above FPE may describe the transmission of the QID signals along a quantum GC by extending the concept of the classical GC for information. The quantum dynamical mutual information formula for the quantum GC can be generally obtained in the coherent state representation,

$$I(A_0(0);B_\alpha(\tau))=\frac{1}{2}\ln\left[1+\frac{(2\pi\mathrm{e})^{\delta(\tau)-1}\sigma_{\mathrm{in}}^{2\delta(\tau)}}{\sigma_{\mathrm{noise}}^2(\tau)}\right]\tag{16}$$

where A_0 (0) is an input ensemble encoded state at time 0 with a special coordinate 0, $B_\alpha(\tau)$ is an output ensemble encoded state at time τ with the coordinate α. σ_{in}^2 and $\sigma_{\mathrm{noise}}^2$ are average power of input signal and noise in the channel, respectively.

Based on the ultimate analysis, we will construct a quantum logical operation or quantum channel between the two nodes as a link to form a quantum network. Because of the "quantum" property, each link between a pair of nodes possesses the probability to open or close. Furthermore, we suppose that there is a new node added into the network stochastically. Each node added to the system at time t_i with an energy ε_i is described by the number of links $k_i(t,t_i,\varepsilon_i)$ at time t. This makes the quantum network similar to the network describing Bose-Einstein condensation. Moreover, it is of interest to allow the $k_i(t,t_i,\varepsilon_i)$ to be also driven by an external field for controlling the final link pattern of the network in the expected level (by administrator). Thus the rate of $k_i(t,t_i,\varepsilon_i)$ with respect to time is expressed as:

$$\begin{aligned}\frac{\partial k_i(t,t_i,\varepsilon_i)}{\partial t}&=m\frac{\mathrm{e}^{-\beta\varepsilon_i}k_i(t,t_i,\varepsilon_i)}{\sum_j\mathrm{e}^{-\beta\varepsilon_j}k_j(t,t_j,\varepsilon_j)}\\&+g[k_i(t,t_i,\varepsilon_i)]\end{aligned}\tag{17}$$

where $g[k_i(t,t_i,\varepsilon_i)]$ is a driving term introduced by the driving field, β is inverse temperature $1/T$, and m is defined as a new node attached by m links to m of the N existing nodes of the network. In general, choosing a different type of driving function can obtain a different type of evolution of $k_i(t,t_i,\varepsilon_i)$. To study the complex behavior of the network resulting from the driven term we choose the following different functions:

(1) Choosing $g[k_i]$ as an exponential function, and exp(k), then we have

$$k_i(t,t_i,\varepsilon_i)=\ln\left[m\frac{f(\varepsilon_i)}{t_i}\left(\frac{t}{t_i}\right)^{f(\varepsilon_i)-1}\right]\tag{18}$$

(2) Choosing g $[k_i]$ as one of seven catastrophic polynomial, such as Elliptic umbilic

$g\left[k_i(t,t_i,\varepsilon_i)\right]=t^3-3ty^2+a(t^2+y^2)+cy+gt$, then if $t\neq a/3$, a solution is given by

$$k_i(t,t_i,\varepsilon_i)=\frac{1}{at_i-3t_it}\left(-\frac{1}{2}t_ic\pm r_1\right)\tag{19}$$

which shows that k_i is type of irrational polynomial of t. The complex behaviors of k_i may be implied by adjusting some parameters and t_i . Our results show that the curve of folds is a parabolic curve around which the number of solutions k_i can be changed. This drives the network to be the type of catastrophe. The connectivity distribution P (k) can be given by the sum of the probabilities P (k) which is a node with an energy ε has a connectivity k. Thus, we have to sum over all the nodes with energy distribution P (ε), which allows us to get complicated P (k) which may have positive exponential, when t = 1.08, when t = 1.08, g = c = 1, a = 5, we have

$$P(k)=\frac{1}{e+k+2.76k^2+3.5}\tag{20}$$

Figure 10 (b) gives $P(k)$ decays with negative exponent of power-law $P(k)$. These motivate us to change k_{i}^{-2} as k_{i}^2 in the corresponding driving terms to get the evolution of $P(k)$ with positive exponent of power-law, when t = 1.08, g = 1, c

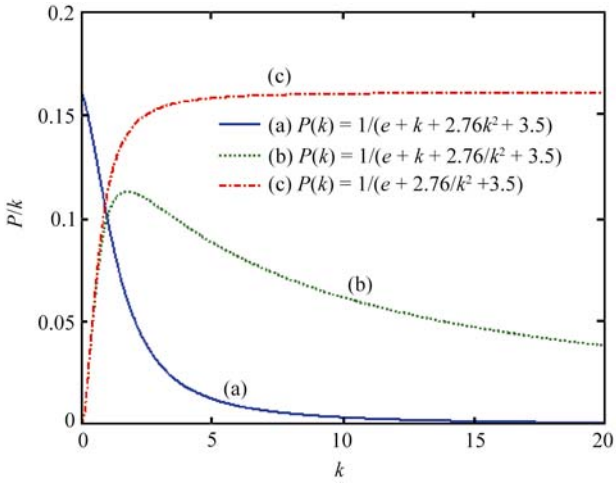

Fig. 10 The degree distribution $P(k)$ vs k.

= 0, a = 5, we have

$$P(k) = \frac{1}{e + 2.76k^{-2} + 3.5} \tag{21}$$

This is shown in Fig.10 (c), which gives a positive exponent of power law $P(k)$. It is seen from Fig.10 that there exist positive and negative exponents of power-laws $P(k)$ if the quantum information network is driven by a kind of catastrophic polynomials.

It is noted that the positive or negative exponent of power-law $P(k)$ can influence the assortativity coefficient r_c of the network. Indeed, if r_c is a quantity corresponding to the correlation coefficient of the degrees of the nodes at the extremes of an edge of the network, $r_c \propto -\langle jk\rangle\langle j\rangle\langle k\rangle$, then from $P(k) = k^{-\gamma} \to k^{\gamma}$, we have

$$\begin{aligned}\langle jk\rangle - \langle j\rangle\langle k\rangle &= k^{-\gamma+3}\left[\frac{1}{-\gamma+3} - \frac{k^{-\gamma+1}}{(-\gamma+2)^2}\right] \\ &\to k^{\gamma+3}\left[\frac{1}{\gamma+3} - \frac{k^{\gamma+1}}{(\gamma+2)^2}\right]\end{aligned} \tag{22}$$

which influences the γ as a function of k and exponent γ of power-law definitely, as shown in Fig.11(a)–(d), which reveal that for the positive exponent of power-law, the γ possesses more stable negative values (correlations) until it tends to $-\infty$, while γ, for the negative exponent of power-law, is positively or negatively unstable and finally tends to 0. All are of negative assortativity. The QIN we proposed may produce positive assortativity r_c as a physical network example, which may help to study QIN having different topological characteristics and mechanism.

This is possibly helpful to find a way to study the different topological characteristics and mechanisms, as well as the inner link and the mechanism that different types of networks possess.

6 Hexagonal nanowire network

Based on the principle of the QIN above, we have also studied the suitability of the hexagonal nanowire network (HNN) [35–37], as shown in Fig.12, to detect the radiation field. This HNN has six levels of transmission for current densities. Suppose an input current density along two arms is $s_1/2$, $s_2/2$, then the output current density with quantum interference to different levels, is as shown.

We apply the idea and the method of the HUHPM to the HNN. The analysis shows that the influence functional phase depends on the final relative velocity of electrons in the arms connected to an output node for a symmetric loop or network. The increase of the order levels of network allows the relative velocity to be increased, which magnifies the effect of quantum interference. The time evolution of the connectivity obeys a power law. The characteristic difference of this network from the bosonic and fermionic network is that the connectivity of the nodes is related to the influence functional phase replace to the energy. All these allow us to study the connectivity distribution by the total hybrid ratio above, i.e., using random/determination preferential attachment. The calculation results reveal that different choice of total hybrid ratio and the related driving function can change the shape of the curve for the degree of distribution $P(k)$ from power law strongly, as shown in Fig.13. These reveal that the topological property change of the microscopic network, such as $k(t)$ or $P(k)$ can influence the dynamic property of the network, such as quantum interference phase. The dynamic characteristics of the network is related to the structure of the topology of the network.

Based on the principle of quantum interference and using nanowires, the HNN can be used to detect the radiation field. The analysis shows that the influence functional phase depends on the final relative velocity of the electrons in the arms connected to an output node for a symmetric loop or network. The increase of order levels of the network allows the relative velocity to be increased, which magnifies the effect of the quantum interference. The time evolution of the connectivity obeys a power law. The characteristic difference of the QIC and HNN from the Bosonic and the Fermionic network is that the connectivity of the nodes is related to the influence functional phase replace to the en-

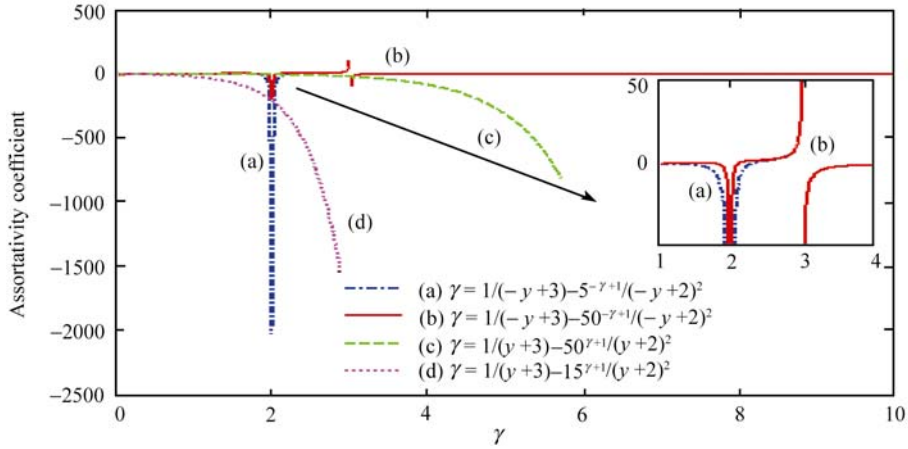

Fig. 11 The assortativity coefficient r_c vs the negative exponent of degree power-law.

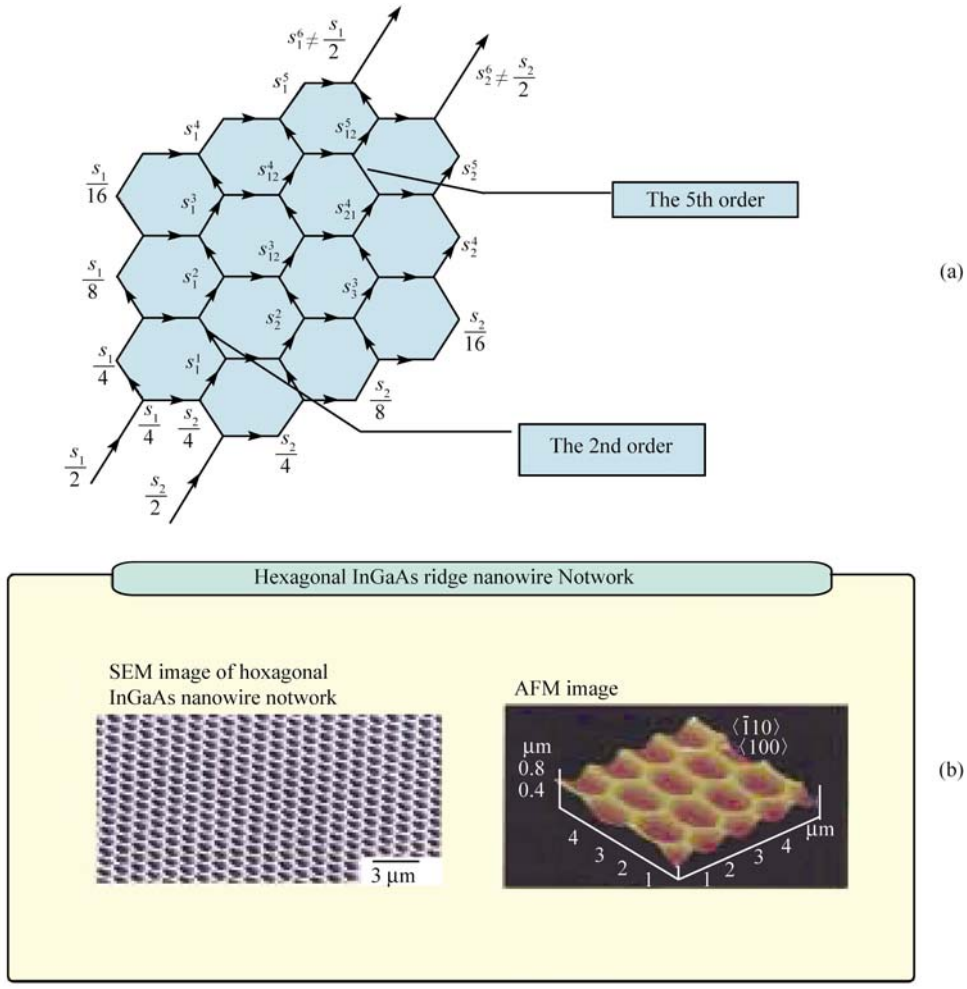

Fig. 12 **(a)** A network consisting of hexagonal nanowire loops. This network has six levels of transmission for current densities. **(b)** The picture of the hexagonal InGaAs ridge nanowire networks.

ergy. All of these allow us to study connectivity distribution by using the idea of a total hybrid ratio of the HUHPM above. The calculation shows that the total hybrid ratio can change the shape of the curve for the connectivity distribution strongly, allowing the network to appear to scale-rich properties, see Fig. 13. These results above for the QIC and the HNN have potential application [37].

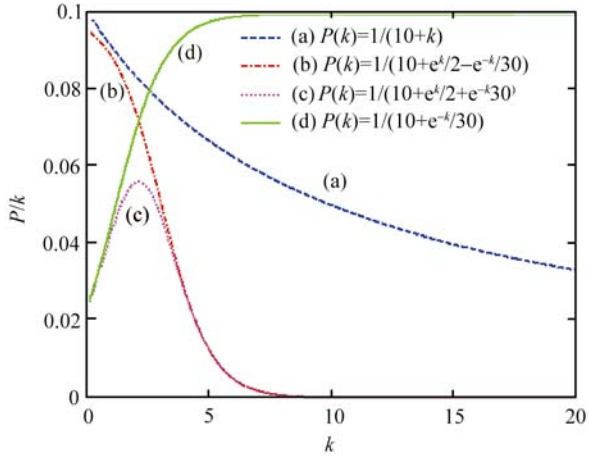

Fig. 13 Several degree power-law distributions in the HNN.

7 Small world model with the same degree of all nodes

The discovery of the SW leads to an avalanche of research on the properties of the SW networks [1]. A much-studied variant of the SW model was proposed by Newman and Watts [2, 38], in which the edges are added between randomly chosen pairs of sites, but no edges are removed from the regular lattice. In 1999, Kasturirangan proposed an alternative model to the SW network [40]. The model starts also with one ring lattice, and then a number of extra nodes are added in the middle of the lattices which are connected to a large number of sites chosen randomly on the main lattice. In fact, even in the case where only one extra node is added, the model shows the SW effect if that node is suffi-

ciently highly connected, which has been solved exactly by Dorogovtsev and Mendes [38]. To investigate the SW effect further, Kleinberg has presented a generalization of the SW model which is based on a two dimensional square lattice [41]. Besides, in order to study other mechanisms for forming the SW networks, Ozik, Hunt and Ott introduced a simple evolution model of growing the small-world networks, in which all connections are made locally to geographically near sites [42].

Generally, SW networks are characterized by three main properties. First, their average path length (APL), which does not increase linearly with the system size, but grows logarithmically with the number of nodes. Second, the average node degree of the network is small. Third, the network has a high average clustering compared to an Erdos-Renyi (ER) random network [43, 44] of equal size and average node degree. The APL can be used to estimate the average transmission delay. One can always reduce the APL by adding more edges, but this could bring in economical and technical pressures. So the average edge number of the nodes must be controlled within an acceptable range. Moreover, the information localizing principle makes the networks with a larger clustering coefficient welcome.

Therefore, the models of SW networks can be diverse in nature and society. We also proposed the model of the same degree (SD) of all the nodes which produces the SW effects very well [44, 45].

To realize the SD-SW model, we suggested two algorithms, one is the so-called "spread all over vertices" (SAV) algorithm [45], the other is the so-called "spread all over boundaries " (SAB) [46] for generating the SW properties from regular ring lattices. During randomly rewiring connections the SAV is used to keep the unchanged number of links. We start with a ring of N nodes, each connected to its k nearest neighbors by undirected edges. For clarity, $N = 10$ and $k = 4$ are taken as the schematic examples here. At each time step we perform one of the following three operations: (i) We randomly select a node i. From the nodes connected with the node i, we randomly select a node j and remove the edge connected to the node i. (ii) From the nodes unconnected with the node i, we randomly select a node u and connect a new edge to the node i. (iii) From the nodes connected with the node u, we randomly select a node v and remove the edge connected to the node u. (iv) For the node v we connect a new edge to the node j.

At each increment of time, four nodes are involved and two original ruled edges are removed, which have never been selected before, two new edges are connected, which will never been changed later. The growth process is repeated until the network grows to the desired percentage. Note that at every step self-connections and duplicate edges are excluded.

The network develops by the successive change based on the above procedure. According to different percentage, which is the proportion of successfully changed node number to the total node number, simulations show that it can generate the SW effect. The approach we propose is similar to the well-known WS model, but the present method is quite different as it leaves the number of connections k of each node unchanged, while the WS algorithm gives rise to a Poisson distribution of connectivity. Leaving k unchanged makes us able to study the effect of rewiring nodes on topological property of these networks.

Comparing the SAV algorithm with the Watts-Strogatz model and the "spread all over boundaries " (SAB) algorithm, three methods can have the same topological properties of the small world networks, as shown in Fig. 14. They have a smaller average path length and larger clustering coefficient. These results offer a diverse formation of the small world networks. One of the advantages for our model is that all the degrees of the nodes are constant but can be selected according to the need. The two algorithms offer a good example of diverse formation of the SW networks since their distribution of node degrees is quite different. Our model may help engineers in the topology-designing and performance analysis of a small world network. It is also useful to research with some applications for the mutual oscillator kinetics inside nodes. It is helpful to the research of some applications for dynamics of mutual oscillator inside nodes and interacting automata associated with networks [46].

We have applied the WS model and the SD model to construct the beam transport network with the small-world effect [47], respectively. We have adopted the global linear coupling control method and the special linear controller to realize the synchronization control of the halo-chaos and periodic state, respectively. It is noted that in our previous

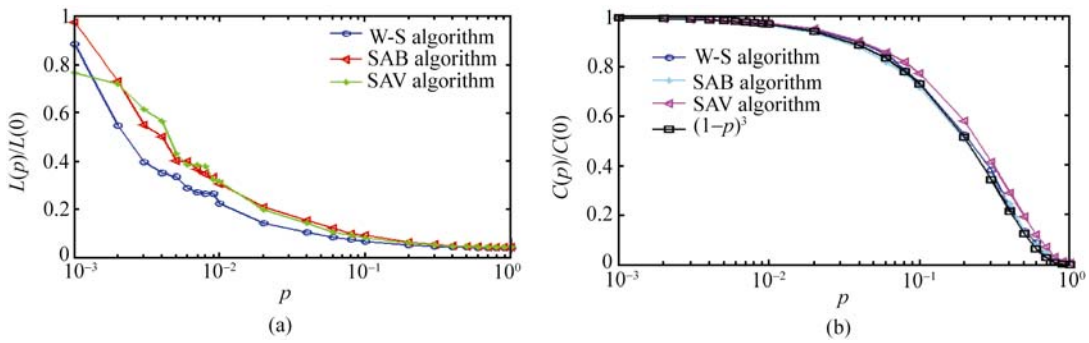

Fig. 14 Comparison of small-world properties for the SAV with WS model [1].

work we have proved that *only nonlinear* feedback control methods can realize the control of the beam halo-chaos in the beam transport network *without any small world topology* [48, 49]. At present, this work demonstrates a very important result; the small world topological properties can affect the dynamics of the beam transport network strongly. If the beam transport network is constructed with the *SW topology, use of special linear feedback method* can easily realize the synchronization control of the beam halo-chaos and periodic states. Therefore, this provides a new idea and a simple effective control of the beam halo-chaos in the high-current accelerator experimental study and the engineering design. It may also be a potential application for halo-chaos secure communication.

8 Summary

Based on the idea of a harmonious unification world, we have developed several theoretical models of network science from the macroscopic to the microscopic levels. These models include a harmonious unifying hybrid preferential model (HUHPM), a large unifying hybrid network model (LUHNM), a quantum interference network (QIN), a hexagonal nanowire network (HNN) and a small-world network with the same degree (SD). Several universal property models and new findings are summarized and reviewed in this article. The HUHPM and the LUHNM can be applied to most un-weighted and weighted complex networks. To clarify these ideas and methods, the HUHPM-BA, the HUHPM-BBV and the HUHPM-TDE are taken as 3 typical models of complex networks, and also extended to study microscopic networks such as the QIC and the HNN. These nontrivial results are useful for investigating the complexity and construction of various theoretical models from the macroscopic to microscopic networks. However, theoretical analysis and application are still open and offers much more challenge for network science researchers.

Acknowledgements This work was financially supported by the key project of the National Natural Science Foundation of China (Grant No. 70431022) and the National Natural Science Foundation of China (Grant No. 70371068). We thank Liu Qiang for drawing figures.

References

1. Watts D. J. and Strogatz S. H., Nature (London), 1998, 393: 440, references therein
2. Newman M. E. J. and Watts D. J., Phys. Lett. A, 1999, 263: 341–346
3. Barabasi A. -L. and Albert R., Science, 1999, 286: 509, references therein
4. Barabasi A. -L., Albert R., and Jeong H., Physica A., 1999, 272: 173
5. http;//newsinfo.nd.edu/,University of Notre Dame, News & Information, August 24, 2006
6. WILSON E O. Consilience—The Unity of Knowledge, Knopf Publishers, Knopf: New York, 1998: 48
7. Strogatz S. H., Nature (London), 2001, 410: 268
8. Albert R., Jeong H., and Barabasi A. -L, Nature (London),1999, 401: 130
9. Albert R. and Barabasi A. L., Rev. Mod. Phys., 2002, 74: 47
10. Albert R., Jeong H., and Barabasi A. -L, Nature (London), 2000, 406: 378
11. Albert R., Jeong H., and Barabasi A. -L., Nature (London), 2001, 409: 542
12. Newman M. E. J., Moore C., and Watts D. J., Phys. Rev. Lett., 2000, 84: 3201
13. Newman M. E. J., Phys. Rev. Lett., 2002,89: 208701;
14. Newman M. E. J., Phys. Rev. E, 2004, 70: 056131
15. Wang W. X., Wang B. H., Hu B., et al., Phys. Rev. E, 2006, 73: 016133
16. Boccaletti S., atora L. V., oreno M. Y., Chavez M., and DU Hwang, Physics Report, 2006, 424(4–5): 175–308
17. WilsonI E. O., Consilience –The Unity of Knowledge, Knopf Publishers, Knopf: New York, 1998: 48
18. Albert R. and Barabasi A. L., Phys. Rev. Lett., 2000, 85: 5234
19. Newman E. J., Strogatz S. H., and Watts D. J., Phys. Rev. E, 2001, 64: 026118
20. Dorogovtsev S. N., and Mendes , Evolution of Networks, Oxford University Press, 2003
21. Dorogovtsev S. N., et al., Phys. Rev. Lett., 2000, 85: 5234
22. Barabasi A. L., Dezso Z., and Bonabeau E., Scientific American, 2003, 288: 60
23. Barrat A., Barthelemy M., and Vespignani A., Phys. Rev. Lett., 2004, 92: 228701
24. Barrat A., Barthelemy M., and Vespignani A., Phys. Rev. E, 2004, 70: 066149
25. Wang W. X., Wang B. H., Hu B., et al., Phys. Rev. Lett., 2005, 94: 188702
26. Fang J. Q. and Liang Y., Chin. Phys. Lett., 2005, 22: 2719
27. Lu X. B., Wang X. F., and Fang J. Q., Physica A, 2006, 371: 841
28. Fang J. Q., Bi Q., Proceedings of The Forth International Conference on Nonlinear Science, Pohang, Korea , 12-14 July 2006: 34
29. Fang J. Q., Bi Q., Li Y., Lu X. B., and Liu Q., Chinese Science, 2006 (in press)
30. Fang J. Q., Bi Q., Li Y., Lu X. B., et al., Advances in Complex Systems, 2006 (accepted)
31. Fang J. Q. and Bi Q., Proceedings of 2006 National Conference on Complex Networks, Wuhan, November 16–18, 2006: 6
32. Bi Q. and Fang J. Q., Chin. Phys. Lett., 2006, 23(7): 1947
33. Bi Q., Fang J. Q., and Aipaip C. W., Physica A, 2006, 371: 409
34. Bi Q., Ruda H. E., and Zhou D. Z., Physica A, 2006, 363 : 198;
35. Bi Q., Ruda H. E., and Zhou D. Z., Physica A, 2006, 364: 170
36. Bi Q. and Fang J. Q., Phys. A , 2006 (accepted)
37. L iug P., Bi Q., and Ruda H. E., J. Appl. Phys, 2006, 99: 094306
38. Newman M. E. J. and Watts D. J., Phys. Rev. E, 1999, 60: 7332
39. Kasturirangan R.,1999, cond-mat/ 9904055
40. Dorogovtsev S. N. and Mendes J. F. F., Europhys. Lett., 2000, 50: 1
41. Kleinberg J., Nature, 2000, 406: 845

42. Ozik J., Hunt B. -R., and Ott E., Phys. Rev. E, 2004, 69: 026108
43. Erdös P., and Rényi A., Publ. Math., 1959, 6: 290
44. P. Erdös and Rényi A., Publ. Math. Ins. Hung. Acad. Sci., 1960, 5: 17
45. Li Y., Fang J. Q., Liu Q., et al., Commun. Theor. Phys., 2006, 45: 67
46. Liu Q., Fang J. Q., Li Y., et al., Complex Systems and Complex Science, 2005, 22: 13
47. Liu Q., Fang J. Q., and Li Y., Commun. Theor. Phys., 2006 (accepted)
48. Fang J. Q., Taming Chaos and developing High-Technology, Beijing: Atomic Energy Press, 2002 (in Chinese)
49. Fang J. Q., Wang Z. S., and Chen G. R., Theor. Phys., 2004, 42: 557